Impact of Color Space on Human Skin Color Detection Using an Intelligent System

HANI K. AL-MOHAIR, JUNITA MOHAMAD-SALEH* AND SHAHREL AZMIN SUANDI
School Of Electrical & Electronic Engineering
Universiti Sains Malaysia
14300 Nibong Tebal, Pulau Pinang
MALAYSIA
jms@eng.usm.my

Abstract: - Skin detection is a primary step in many applications such as face detection and online pornography filtering. Due to the robustness of color as a feature of human skin, skin detection techniques based on skin color information have gained much attention recently. Many researches have been done on skin color detection over the last years. However, there is no consensus on what color space is the most appropriate for skin color detection. Several comparisons between different color spaces used for skin detection are made, but one important question still remains unanswered is, "what is the best color space for skin detection. In this paper, a comprehensive comparative study using the Multi Layer Perceptron neural network MLP is used to investigate the effect of color-spaces on overall performance of skin detection. To increase the accuracy of skin detection the median filter and the elimination steps are implemented for all color spaces. The experimental results showed that the YIQ color space gives the highest separability between skin and non-skin pixels among the different color spaces tested.

Key-Words: - skin detection, color-space, Neural Network

1 Introduction

Image segmentation is a process of dividing an image into non-overlapping regions consisting of groups of connected homogeneous pixels. Typical parameters that define the homogeneity of a region in a segmentation process are color, depth of layers, gray levels, texture, etc [1]. A good example of image segmentation is skin detection which is achieved by classifying the image pixels into two groups; skin pixels and non-skin pixels using skin color information. The process of utilizing skin color information as a cue in skin detection techniques has gained much attention because skin color provides computationally effective yet, robust information against rotations, scaling and partial occlusions [2]. Skin color detection is primarily an important process in applications such as face detection [3-5], gesture analysis [6], Internet pornographic image filtering [7], surveillance systems [8]. Figure 1 illustrates a general example of exploiting skin color for face detection. In this case, face detection is achieved by extracting the common face features, and utilizing skin color detection as primary steps to minimize the area from which the face features are extracted. As a result, the necessary time for accomplishing face detection can be minimized significantly.

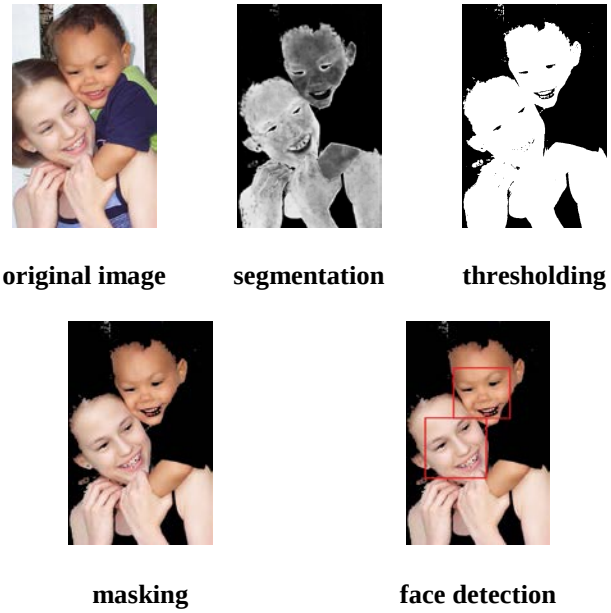

Fig. 1 Example of face detection process utilizing skin color detection

In order to make use of skin color information, many researches have been directed to understanding its characteristics. Research analysis has shown that human skin color has a restricted

ISBN: 978-960-474-350-6

range of hues and is not deeply saturated, as the appearance of skin is formed by a combination of blood (red) and melanin (brown, yellow) [10]. Therefore, human skin color does not fall randomly in a given color space, but rather clustered within a small area in the color space. Several studies have shown that the major difference in skin color among different people lies largely in their intensity rather than in their chrominance [11]. Thus, if an image is first converted into a color space, which provides a separation of luminance channel and two chrominance components like the normalized (r, g, b) color space, then skin-like regions can easily be detected [12]. Numerous algorithms have been proposed for skin detection during the past few years. However, skin color detection can be a very challenging task as the skin color in an image is sensitive to various factors such as illumination conditions, camera characteristics and ethnicity [2].

In this study the MLP which is a universal classifier is used to optimize the overall performance of different color-spaces used in skin detection by comparing the higher skin detection rates with low false positives. The goal of this paper is to present and evaluate various color spaces used in skin detection to find the optimal color space using ECU database. Multi Layer Perceptron artificial neural network system (MLP) is used for skin color classification, moreover to describe and evaluate the color spaces characteristics and performance. The paper is arranged as follows. Section 2 introduces the different color spaces used for skin color detection. Section 3 covers preparing the training data set. Section 4 explains the methodology of this work. Section 5 gives the experiment results and Section 6 concludes the paper

2 Color Spaces

Color is a significant source of information for a wide range of research areas such as segmentation, image analysis classification, and object recognition. However, some of the original colors in an image might not be appropriate for analysis, and the colors must be adjusted. Adjusting the colors can be done by transferring colors from space to another, while preserving the image's original details and natural look at the same time [13]. Skin detection process involves two major steps which are; (1) to represent the image using a proper color space, (2) to model the skin and non-skin pixels using inference methodology to obtain information from available skin samples and to extrapolate the results to given samples [2, 14]. Selecting proper color space is crucial for skin color detection. In relation to this, how is optimal color space for skin-classification estimated? Several comparisons between different color spaces used for skin detection can be found in the literature [14-23], but one important question still remains unanswered is, “what is the best color space for skin detection?” Many authors do not provide strict justification of their color space choice [13]. Some of them cannot explain the contradicting results between their experiments or experiments reported by others [22]. Moreover, some authors think that selecting a specific color space is more related to personal taste rather than experimental evidences [14, 24]. However, the most common result of the researches obtain on the effect of color space on skin detection is that different modeling methods react very differently on the color space change [2, 13]. This paper will present a comprehensive experiment to introduce the best color space used in skin detection using the MLP. The details of color spaces used in this study are as follows:

2.1 RGB

Colors are specified in terms of the three primary colors red (R), green (G) and blue (B). It is an additive model because all colors are created from these primary colors combining them in various ways. For example, red (255, 0, 0) and green (0, 255, 0) combined in equal amounts create yellow: (255, 255, 0). the amount of each primary color gives its intensity. If all components are of highest intensity, then the color white results. This is the most extended and used color format because it is the one used in displays technology, but nowadays it is not the most used in skin detection, because it is not very robust when light conditions changes [25]

2.2 Normalized RGB

RGB correspond to three primary colors: red, green and blue. It is one of the most widely used color spaces for processing and storing digital image data. In order to reduce the dependence on lighting, the RGB values are normalized by a simple normalization procedure as follows.

$$r = \frac{R}{R+G+B} \quad (1)$$

$$g = \frac{g}{R+G+B} \quad (2)$$

$$b = \frac{b}{R+G+B} \quad (3)$$

ISBN: 978-960-474-350-6

The sum of the normalized components of RGB is unity (r + g + b = 1), and it means that r and g values are enough to represent this color space as the third component, b, can be calculated directly based on r and g. The RGB and its normalized version are among the popular color spaces used for skin detection and have been commonly used [4, 12, 26-30].

2.3 YCbCr

The YCbCr color space is commonly used by European Television Studios. It is supposed to reduce the redundancy present in RGB color channels and represent the color with statistically independent components [2]. The YCbCr represents the color by luminance, Y, and chrominance as the difference between two colors, Cr and Cb using the following set of equations [13]:

$$Y = 0.299R + 0.587G + 0.114B \quad (4)$$

$$C_b = B - Y \quad (5)$$

$$C_r = R - Y \quad (6)$$

Compared to the RGB color space, YCbCr has an explicit separation of luminance and chrominance components, which makes it very attractive for skin detection [4, 15,31-35, 36].

2.4 YIQ

The YIQ color space is similar to YCbCr color space as they belong to the same category of orthogonal color spaces [2]. The luminance is represented by Y, and the chrominance is represented by I and Q. The I value describes the change from orange to cyan, while Q describes the change from purple to yellow-green. Transforming RGB color space into YIQ color space allows separating the luminance information from hue. This effective separation of information makes the YIQ color space useful for skin color detection [28,37-38]. The following set of equations is used to transform RGB into YIQ [39]:

$$Y = 0.299R + 0.587G + 0.114B \quad (7)$$

$$I = 0.596R - 0.275G - 0.321B \quad (8)$$

$$Q = 0.212R - 0.523G + 0.311B \quad (9)$$

2.5 HSV

Hue-saturation-value color-space was introduced when there was a need for the user to specify color properties numerically. They describe color with intuitive values, based on the artist's idea of tint, saturation and tone. Hue defines the dominant color (such as red, green, purple and yellow) of an area; saturation measures the colorfulness of an area in proportion to its brightness. The value is related to the color luminance. The following set of equations is used to transform RGB into HSV[40]:

$$H = \arccos \frac{\frac{1}{2}((R-G)+(R-B))}{\sqrt{((R-G)^2+(R-B)(G-B)}} \quad (10)$$

$$S = 1 - 3\frac{\min(R,G,B)}{R+G+B} \quad (11)$$

$$V = \frac{1}{3}(R+G+B) \quad (12)$$

2.6 YUV

This model defines a color space in terms of one luminance (Y channel) and two chrominance components (UV channels). U represents the color difference between blue signal and luminance (B − Y) and V represents the difference between red and luminance (R − Y). YUV is used for analog television such as PAL or NTSC. Human vision is much more sensitive to luminance variations than chrominance variations. YUV codification takes advantages of this fact, giving more bandwidth to luminance so that the color space goes closer to human perception (although YUV is not as close as HSV color space). YUV signals are created from an original RGB (red, green and blue) source. The weighted values of R, G and B are added together to produce a single Y signal, representing the overall brightness, or luminance, of that point. The U signal is then created by subtracting the Y from the blue signal of the original RGB, and then scaling; and V by subtracting the Y from the red, and then scaling by a different factor. Therefore, conversions between RGB and YUV formats can be done through linear transformations as follows [25]:

$$Y = 0.299R + 0.587G + 0.114B \quad (13)$$

$$U = -0.14713R - 0.28886G + 0.436B \quad (14)$$

$$V = 0.615R - 0.51499G - 0.10001B \quad (15)$$

2.7 YDbDr

This color space is very similar to the previous ones: it is very close to YUV and it is related with color spaces such as YIQ, YPbPr and YCbCr. YDbDr color space is composed of three components: Y, Db and Dr. Y channel represents the luminance

ISBN: 978-960-474-350-6

information, while Db and Dr are the chrominance components (representing the blue and the red color differences respectively). As with the previous models, transformations between YDbDr and RGB are linear, and they are performed using the following expressions[41]:

$$Y = 0.299R + 0.587G + 0.114B \quad (16)$$

$$Db = -0.450R - 0.883G + 1.333B \quad (17)$$

$$Dr = -1.333R + 1.116G + 0.217B \quad (18)$$

2.8 CIE L*a*b

The three coordinates of this color model present the lightness of the color (L* = 0 yields black and L* = 100 indicates diffuse white), its position between red/magenta and green (a*, negative values indicate green while positive values indicate magenta) and its position between yellow and blue (b*, negative values indicate blue and positive values indicate yellow). The L* coordinates ranges from 0 to 100. The possible range of a* and b* coordinates is independent of the color space that one is transforming from, since the conversion below uses X and Y which come from RGB [69].

$$L^* = 116 \times f\left(\frac{Y}{Y_n}\right) - 16 \quad (19)$$

$$a^* = 500 \times \left[f\left(\frac{X}{X_n}\right) - f\left(\frac{Y}{Y_n}\right) \right] \quad (20)$$

$$b^* = 200 \times \left[f\left(\frac{Y}{Y_n}\right) - f\left(\frac{Z}{Z_n}\right) \right] \quad (21)$$

$$f(t) = \begin{cases} t^{1/3} \; if \; t > \left(\frac{6}{29}\right)^3 \\ \frac{1}{3}\left(\frac{29}{6}\right)^2 t + \frac{4}{29} \; o.w. \end{cases} \quad (22)$$

where X_n, Y_n and Z_n are CIE XYZ normalized values of the reference white point.

3 Preparing the training dataset

In this work two datasets have been used, one for training and one for testing. For preparing the training dataset, we have collected 150 images of skin pixels and 150 images of non-skin pixels. The 150 images that contain the human skin are downloaded from the "Humanae Project" webpage. Humanae is a chromatic inventory, which is a project that reflects on the colors beyond the borders of the codes by referencing the pantone color scheme. Pantone Guides are one of the main color classification systems, which are represented by an alphanumeric code, allowing to accurately recreating any of them in any media. It is a technical industrial standard often called real color [42]. The Humanae dataset contains a wide range of images of people of different genders, races, and ages. Besides the diversity, the images of Humanae dataset are of quite high resolution compared to Compaq dataset [29].

For each image in the skin pixels group , 5 blocks of size 40x40 pixels were selected manually from different areas of the image as shown in Figure 2. The blocks were selected from, forehead, cheeks, shoulders, or chest. The reason behind that is to take into consideration any little differences in skin color tone that may exist between the different body areas of the same person. As a result, 8000 skin pixels were collected from each image (40*40*5). So the total number of skin pixels that were collected from the images is 1.2 million pixels.

Another 1.2 million non-skin pixels were collected from the non-skin group of 150 images downloaded from the internet which contains no human skin. Using the equations mentioned in section 2, the resultant dataset (2.4 million pixels) were transformed from the RGB color space to the targeted color spaces, YCbCr, YDbDr, YIQ, YUV, HSV, normalized RGB, and Lab. So, eight different data sets were obtained and ready to be used for training the neural network.

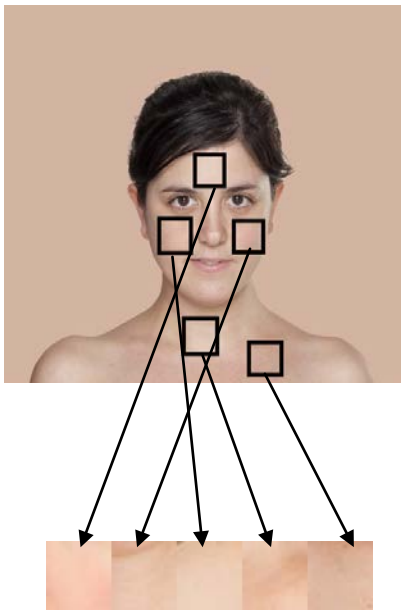

Fig. 2 Blocks Extracted for Training from Humanae Dataset [42]

For testing the trained neural network, 800 images (212,472,234 pixels) randomly selected from the ECU image database [43], have been used. Images of the database contain skin pixels belonging to persons of different origins, with unconstrained illumination and background conditions, which make the evaluation of the color space used in skin detection task more challenging and difficult.

4 Methodology

In the first stage, the prepared data set is used for training the NN. In the second stage, the trained NN is used to detect the skin in the selected images of ECU data set.

4.1 Training the NN

The 2.4 million pixels which represent the data set have been used for training the dataset. The training data is divided into three subsets: Training 70%, validation 15%, and testing 15%. Multi Layer Neural Network simulates a back propagation training algorithm that is a well-known algorithm widely used in artificial intelligence. An ANN consists of at least three layers of units: an input layer, at least one intermediate hidden layer, and an output layer. Typically, units are connected in a feed-forward fashion with input units fully connected to units in the hidden layer and hidden units fully connected to units in the output layer. When a MLP network is cycled, an input pattern is propagated forward to the output units through the intervening input-to-hidden and hidden-to-output weights. The neurons are interconnected in such a way that information relevant to the I/O mapping is stored in the weights [12]. Fig. 3 shows the architecture of the ANN which has been used.

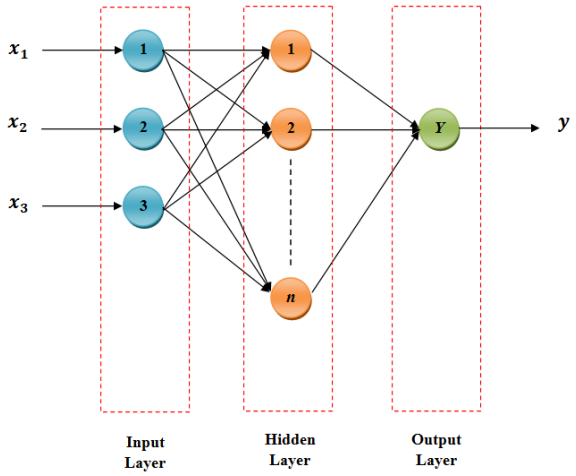

Fig. 3 MLP Neural Network Architecture

In this work the MLP has been implemented using MATLAB Neural Network Toolbox 7.0. with different numbers of neurons in the hidden layer. For each configuration, the training process was repeated for 20 times trying to find the best performance of the network in terms of minimum mean square error (MSE). Table 1 shows the results of the training phase for the different color spaces used. The table illustrates that the best performance can be achieved using YCbCr color space with 15 neurons in the hidden layer.

Table. 1 Best validation performance (MSE)

Color Space	Number of neurons (in hidden layer)	Best validation performance (mse)
RGB	8	0.099
norRGB	15	0.118
YCbCr	15	0.098
YDbDr	15	0.099
YIQ	15	0.099
YUV	12	0.100
LAB	15	0.100
HSV	12	0.097

4.2 Testing the NN

The conventional scenario to test the trained NN is to convert the testing images into the targeted color space and the resultant data is applied to the NN. Then, a the threshold is used to convert the output of the NN into binary form (0 or 1). In the obtained binary image, the 1 values represents skin pixels while 0 represents non-skin values.

In order to enhance the accuracy of detection, we add two steps. First, a median filter is used in order to eliminate the false positive pixels that appear like noise in the output of NN. However, after applying the threshold, some small false positive areas still exist. The second step to increase the accuracy is to measure the size (in pixels) of all detected skin areas, and those areas which with sizes less than 5% of the largest skin area in the image are neglected. The whole process of skin detection is illustrated in Fig. 4.

5 Results

The ECU data set was used for testing the trained ANN and different thresholds have been tested to

ISBN: 978-960-474-350-6

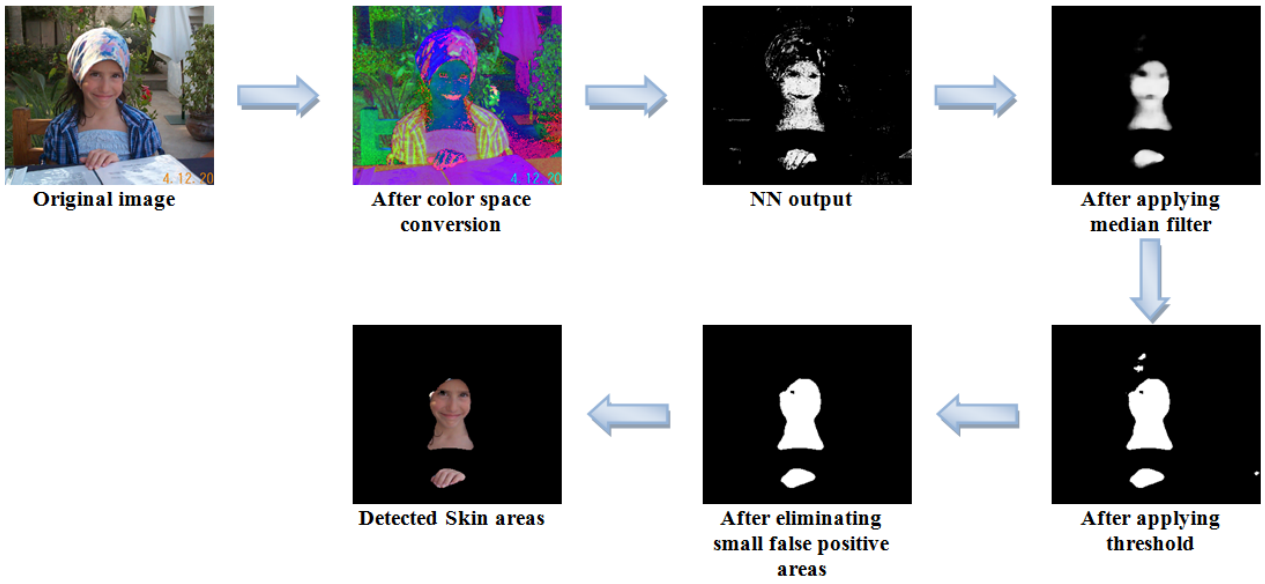

Fig. 4 The process of skin detetcion

optimize the results. The confusion matrix was used to represent the actual and predicted classifications done by the network as shown in Fig. 5. The performance of such an ANN is commonly evaluated using the data in the matrix [44].

The overall performance of the trained ANN is measured by the accuracy (*AC*), which is the proportion of the total number of predictions that were correct. However, the overall accuracy *AC* calculated as shown above may not be an adequate performance measure when the dataset is imbalanced, i.e. the number of negative cases is much greater than the number of positive cases [45]. Suppose there are 1000 pixels, 995 of which are skin pixels and 5 of which are non-skin pixels. If the ANN classifies them all as non-skin pixels, the accuracy would be 99.5%, even though the classifier missed all skin pixels. Other performance measures account for this by including *TP* in a product as in *F-Measure* [46], as defined in equation 23.

$$F1 = \frac{(\beta^2 + 1) * P * TP}{\beta^2 * P + TP} \qquad (23)$$

where β has a value from 0 to infinity and is used to control the weight assigned to *TP* and *P*. Fig. 6 illustrates that F-*Measure* can reflect the accuracy better than *AC*. The skin area is about 3% of the image and it can be detected completely (*TP* ratio = 98%). The non-skin area, which is mistakenly detected as skin area, is larger than the true skin area and one can expect that the *FP* is quite high. However, the *FP* ratio = 9% because the skin area is very small compared to the non-skin area. The accuracy for this example is *AC* = 91.21% which does not reflect the real situation. On the other hand, *P* = 26% which means that only 26% of the area detected as skin is true skin. The accuracy for this example measured by *F-Measure* is *F1* = 41.92 % which reflects the real situation.

AC : Accuracy
TP : True positive
TN : True negative
P : Precision

		Truth Data			
		Skin	non-Skin	Classification overall	Producer Accuracy (Precision)
Classifier Data	skin	a	b	$a+b$	$P = \frac{a}{a+b}$
	non-Skin	c	d	$c+d$	$\frac{d}{c+d}$
	Truth overall	$a+c$	$b+d$	$a+b+c+d$	
	User Accuracy (Recall)	$TP = \frac{a}{a+c}$	$TN = \frac{d}{b+d}$		
	Overall Accuracy	$AC = \frac{a+d}{a+b+c+d}$			

Fig. 5 Confusion matrix

A comparison between the eight color spaces in terms of *TP*, *FP*, *P*, *AC*, and *F* is presented in Table 2 (without the median filter and the elimination steps) and in Table 3 (with the median filter and the elimination steps). Another comparison between the eight color spaces is presented in Fig. 7.

ISBN: 978-960-474-350-6

6 Discussion

Artificial Neural Networks have been adopted for enhancing the separability between skin and non-skin pixels benefitting from their flexibility and ability to adapt to the various illumination conditions and background characteristics. Many color space can be used for representing color images, and researchers have compared between the impact of color space used on the accuracy of human skin detection. Nevertheless, there is no such a consensus on what color space that can achieve the highest accuracy of detection. The reason behind that may be the wide range of detection algorithms that have been used in comparing between color spaces. In other words, there is no an optimum color space that may be used to achieve the best accuracy with any detection algorithm. For a specific detection technique, there is one or two color spaces which may be achieve the most efficient and accurate detection. Based on that, and knowing that the previous comparisons between color spaces have not been carried out using ANN, this paper adopted ANN for comparison.

Original image

Skin areas (Ground truth)

Skin areas (detected)
***F-Measure* = 41.92%, *AC* = 91.21%**

Fig. 6 The difference between *F-Measure* and *AC*

Different color spaces have been used for the comparison in this paper, and different numbers of neurons in the hidden layer have been exploited. During the training process, all the color spaces, except HSV, have almost the same performance in terms of MSE as shown in Table 1. When the trained networks used for evaluation, all the color spaces, except norRGB, have almost the same accuracy with a little bit of variation as shown in Tables 2 and 3. When no median filter and elimination steps are used, the accuracy ranges from 71.27% to 75.24%. Adding the median filter and the elimination steps increases the accuracy for all color spaces, and makes variation lower; 74.27% to 77.83%. The median filter the elimination steps enhanced the accuracy by increasing the *TP* and *P* and by reducing the *FP* ratios. However, the YIQ has the most accurate detection measured by *F1-measure*.

Although, the results of this study reveals impact of color spaces on the accuracy of skin color detection using ANN, it emphasizes that pixels color information is not enough to achieve an accurate separability between skin and non-skin pixels. This can be noticed form the average accuracy achieved in this study. To enhance the accuracy of skin detection we suggest exploiting texture along with color to distinguish between skin and non-skin areas of an image. A wide range of texture descriptors such as statistical or histogram edge descriptors, or much more sophisticated descriptors such as Gabor filters, may be employed in order to achieve the highest accuracy.

7 Conclusions

Skin detection is an important process in many of computer vision systems. Color space information is assumed to have an impact on increasing the separability between skin and non-skin pixels. In this paper, we compared between 8 color spaces for skin detection using the MLP neural network. Among the different color spaces, the experimental results showed that the YIQ color space gives the highest separability between skin and non-skin pixels measured by *F1-measure*. Moreover, adding the median filter and the elimination steps increases the accuracy for all color spaces. However, the overall results emphasize that pixels color information cannot be used alone to achieve accurate skin detection. Combining color and texture may lead to much more accurate and efficient skin detection.

ISBN: 978-960-474-350-6

Color Space	*Th* (threshold)	*TP* (%)	*FP* (%)	*P* (%)	*F1-measure* (%)
RGB	**0.08**	**78.27**	**6.22**	**69.15**	**73.43**
NorRGB	**0.22**	**78.32**	**12.05**	**53.65**	**63.68**
YCbCr	**0.08**	**78.43**	**5.63**	**71.26**	**74.67**
YDbDr	**0.06**	**78.87**	**5.97**	**70.19**	**74.27**
YIQ	**0.06**	**80.05**	**5.98**	**70.98**	**75.24**
YUV	**0.1**	**77.56**	**7.14**	**65.92**	**71.27**
LAB	**0.08**	**79.15**	**6.41**	**68.73**	**73.57**
HSV	**0.04**	**80.20**	**7.16**	**67.29**	**73.18**

Table 2: Average accuracy measured by *F1-measure*
(Without the median filter and the elimination steps)

Color Space	*Th* (threshold)	*TP* (%)	*FP* (%)	*P* (%)	*F1-measure* (%)
RGB	**0.08**	**79.52**	**5.20**	**73.75**	**76.53**
NorRGB	**0.22**	**76.50**	**8.65**	**61.88**	**68.42**
YCbCr	**0.08**	**78.83**	**4.49**	**76.31**	**77.55**
YDbDr	**0.06**	**79.23**	**4.80**	**75.19**	**77.16**
YIQ	**0.06**	**80.43**	**4.82**	**75.39**	**77.83**
YUV	**0.1**	**79.15**	**6.24**	**69.97**	**74.27**
LAB	**0.08**	**78.65**	**4.86**	**74.80**	**76.68**
HSV	**0.04**	**80.83**	**5.80**	**71.89**	**76.10**

Table 3: Average accuracy measured by *F1-measure*
(With the median filter and the elimination steps)

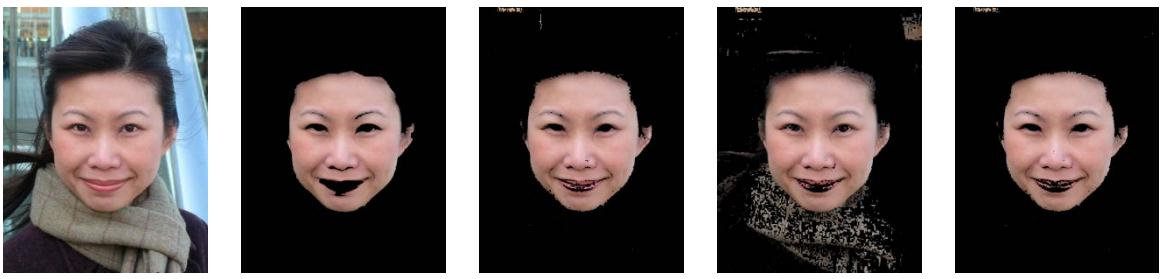

Original image | **Ground truth** | **RGB** *F1* **= 96.34%** | **norRGB** *F1***= 78.89%** | **YCbCr** *F1***= 96.94%**

YDbDr *F1***= 96.18%** | **YIQ** *F1***= 96.59%** | **YUV** *F1***= 96.31%** | **Lab** *F1***= 96.76%** | **HSV** *F1***= 96.647%**

Fig. 7 Skin detection using the different color spaces for an image from ECU dataset

ISBN: 978-960-474-350-6

References:

[1] C. C. Liu and P. C. Chung, Objects extraction algorithm of color image using adaptive forecasting filters created automatically, International Journal of Innovative Computing, Information and Control, vol.7, no.10, pp.5771-5787, 2011.

[2] P. Kakumanu, , S. Makrogiannis, and N. Bourbakis, A survey of skin-color modeling and detection methods, Pattern Recognition, vol.40, no.3, pp.1106-1122, 2007.

[3] C. Zhipeng, H. Junda and Z. Wenbin, Face detection system based on skin color model, 2nd International Conference on Networking and Digital Society (ICNDS), vol.2, pp.664-667, 2010.

[4] J. M. Chaves-Gonzalez, M. A. Vega-Rodriguez, J. A. Gomez-Pulido and J. M. Sanchez-Perez , Detecting skin in face recognition systems: A colour spaces study, Digital Signal Processing, vol.20, no.3, pp.806-823, 2010.

[5] Z. Zakaria, N. A. Isa and S. A. Suandi, Combining Skin Colour and Neural Network for Multiface Detection in Static Images, Symposium on Information & Communication Technology (SPICT09), Kuala Lumpur, pp.147-154, 2009.

[6] J. Han, G. Awad and A. Sutherland, Automatic skin segmentation and tracking in sign language recognition, Computer Vision, IET, vol.3, no.1, pp.24-35, 2009.

[7] J. S. Lee, Y. M. Kuo and P. C. Chung, Detecting Nakedness in Color Images. Intelligent Multimedia Analysis for Security Applications, Springer Berlin , Heidelberg SCI 282, pp. 225-236, 2010.

[8] Z. Zhang, H. Gunes, and M. Piccardi, Head detection for video surveillance based on categorical hair and skin colour models, 16th IEEE International Conference on Image Processing (ICIP), pp.1137-1140, 2009.

[9] M. Rasheed , Face Detection based on Skin colour point pixel processing using OpenCV [cited 2012 January 20], Available from: http://aspilham.blogspot.com/2011/01/face-detection-based-on-skin-colour.html.

[10] M. M. Fleck, D. A. Forsyth and C. Bregler, Finding Naked People, 4th European Conference on Computer Vision, Cambridge, UK, pp.593-602, 1996.

[11] J. Yang and A. Waibel, A real-time face tracker, Proceedings of the 3rd IEEE Workshop on Applications of Computer Vision (WACV '96), pp.142-147, 1996.

[12] L. Chen, J. Zhou, Z. Lid, W. Chen and G. Xiong, A skin detector based on neural network, IEEE International Conference on Communications, Circuits and Systems, vol.1, pp.615-619, 2002.

[13] C. C. Liu, A Global Color Transfer Scheme Between Images Based On Multiple Regression Analysis, International Journal of Innovative Computing, Information and Control, vol.8, no.1A, pp.167-186, 2012.

[14] A. Abadpour and S. Kasaei, Comprehensive Evaluation of the Pixel-Based Skin Detection Approach for Pornography Filtering in the Internet Resources, International Symposium on Telecommunications, IST, pp.829-834, 2005.

[15] B. D. Zarit, B. J Super and F. K. Quek, Comparison of Five Color Models in Skin Pixel Classification, Proceedings of the International Workshop on Recognition, Analysis, and Tracking of Faces and Gestures in Real-Time Systems, pp.58-63, 1999.

[16] J. C. Terrillon and S. Akamatsu, Comparative Performance of Different Skin Chrominance Models and Chrominance Spaces for the Automatic Detection of Human Faces in Color Images, Proceedings of the Fourth IEEE International Conference on Automatic Face and Gesture Recognition, pp.54-61, 2000.

[17] G. Gomez, On selecting colour components for skin detection, 16th International Conference on Pattern Recognition, pp.961-964, 2002.

[18] G. Gomez and E. F. Morales, Automatic Feature Construction and a Simple Rule Induction Algorithm for Skin Detection, The ICML Workshop on Machine Learning in Computer Vision, 2002.

[19] H. Stern and B. Efros, Adaptive Color Space Switching for Face Tracking in Multi-Colored Lighting Environments, Proceedings of the Fifth IEEE International Conference on Automatic Face and Gesture Recognition, pp.249-254, 2002.

[20] M. C. Shin, K. I. Chang and L. V. Tsap, Does colorspace transformation make any difference on skin detection?, Sixth IEEE Workshop on Applications of Computer Vision (WACV), pp.275-279, 2002.

[21] S. Jayaram, S. Schmugge , M. C. Shin and L. V. Tsap, Effect of colorspace transformation, the illuminance component, and color modeling on skin detection. Computer Vision and Pattern Recognition (CVPR), 2004.

[22] D. Kuiaski, H. V. Neto, G. Borba and H. Gamba, A Study of the Effect of Illumination Conditions and Color Spaces on Skin Segmentation, Computer Graphics and Image Processing (SIBGRAPI), pp.245-252, 2009.

[23] S. L. Phung, A. Bouzerdoum and D. Chai, Skin segmentation using color pixel classification: analysis and comparison, IEEE Transactions on Pattern Analysis and Machine Intelligence , vol.27, no.1, pp.148-154, 2005.

[24] M. H. Yang, D. J. Kriegman and N. Ahuja, Detecting faces in images: a survey, IEEE Transactions on Pattern Analysis and Machine Intelligence, vol.24, no.1, pp.34-58, 2002.

[25] J. M. Chaves-Gonzlez , M. A. Vega-Rodguez, J. A. Gomez-Pulido and J. M. Snchez-Pérez, Detecting skin in face recognition systems: A colour spaces study, Digital Signal Processing pp. 806–823,2010.

[26] M. J. Seow, D. Valaparla and V. K. Asari, Neural network based skin color model for face detection, Applied Imagery Pattern Recognition Workshop, pp.141-145, 2003.

[27] K. K. Bhoyar and O. G. Kakde, Skin Color Detection Model Using Neural Networks and its Performance Evaluation, Journal of Computer Science, vol.6, no.9, pp.963-968, 2010.

[28] J. Brand and J. S. Mason, A comparative assessment of three approaches to pixel-level human skin-detection, 15th International Conference on Pattern Recognition Proceedings, pp.1056-1059, 2000.

[29] M. J. Jones and J. M. Rehg, Statistical color models with application to skin detection, IEEE Computer Society Conference on Computer Vision and Pattern Recognition, vol.1, 1999.

[30] Y. Tu, F. Yi., G. Chen, S. Jiang and Z. Huang, Skin color detection by illumination estimation and normalization in shadow regions, IEEE International Conference on Information and Automation (ICIA), pp.1082-1085, 2010.

[31] H. Rein-Lien, M. Abdel-Mottaleb and A.K. Jain, Face detection in color images, IEEE Transactions on Pattern Analysis and Machine Intelligence, vol.24, no.5, pp.696-706, 2002.

[32] S. L. Phung, A. Bouzerdoum and D. Chai, A novel skin color model in YCbCr color space and its application to human face detection, International Conference on Image Processing. vol.1, pp.289-292, 2002.

[33] G. Yang, H. Li, L. Zhang and Y. Cao, Research on a Skin Color Detection Algorithm Based on Self-adaptive Skin Color Model, Communications and Intelligence Information Security (ICCIIS), pp.266-270, 2010.

[34] A. A. Zaidan, N. N Ahmad, H. Abdul Karim, G. M. Alam and B. B. Zaidan, Increase reliability for skin detector using backprobgation neural network and heuristic backprobgation neural network and heuristic, Scientific Research and Essays, vol.5, no.19, pp.2931-2946, 2010.

[35] C. A. Doukim, J. A. Dargham, A. Chekima and S. Omatu, Combining Neural Networks For Skin Detection , An International Journal (SIPIJ), vol.1, no.2, pp.1-11, 2011.

[36] M. Zhao and Y. Zhao, Skin Color Segmentation Based on Improved 2D Otsu and YCgCr. International Conference on Electrical and Control Engineering (ICECE), pp.1954-1957, 2010

[37] L. Duan, Z. Lin, J. Miao and Y. Qiao, A Method of Human Skin Region Detection Based on PCNN, Advances in Neural Networks , pp.486-493, 2009.

[38] Y. Dai and Y. Nakano, Face-texture model based on SGLD and its application in face detection in a color scene, Pattern Recognition, vol.29, no.6, pp.1007-1017, 1996.

[39] D. Chai, S. L. Phung, and A. Bouzerdoum, A Bayesian skin/non-skin color classifier using non-parametric density estimation, International Symposium on Circuits and Systems, ISCAS, vol.2, pp.464-467, 2003.

[40] V. Vezhnevets, V. Sazonov and A. Andreeva, A Survey on Pixel-Based Skin Color Detection Techniques, Proceedings of the GraphiCon, pp.85-92, 2003.

[41] Shi, Yun Q. and Sun, Huifang Image and Video Compression for Multimedia Engineering, CRC Press, 2000

[42] (http://humanae.tumblr.com/

[43] S.L. Phung, A. Bouzerdoum, D. Chai, Skin segmentation using color pixel classification: analysis and comparison, IEEE Trans. Pattern Anal. Mach. Intell. 27 (1) (2005)

[44] http://www2.cs.uregina.ca/~dbd/cs831/notes/confusion_matrix/confusion_matrix.html

[45] Chawla, Nitesh V. "Data mining for imbalanced datasets: An overview." In Data mining and knowledge discovery handbook, pp. 853-867. Springer US, 2005.

[46] Lewis, David, and William Gale. "Training text classifiers by uncertainty sampling." (1994).